P-986 Addendum 2: Physics Studies

P-986 Collaboration

May 26, 2009

Abstract

1 Introduction

We have studied the performance of a simple $\bar{p}p$ experiment based on the E835 lead-glass barrel calorimeter with an inserted solenoidal magnetic spectrometer. We consider the proposed apparatus configuration shown in Fig. 1. Key parameters of the simulations are given in Table 1. We discuss the response and physics reach of this detector configuration for charm and $X(3872)$ studies. Since it is crucial to these studies, we first review the capabilities of the Fermilab Antiproton Source as compared with other similar facilities.

2 Fermilab Antiproton Source

The Fermilab Antiproton Source is the most productive in the world, now and for the foreseeable future. The CERN Antiproton Decelerator (AD) is the only other operating antiproton source. The AD is designed to deliver very low energy antiprotons for stopping physics; $\approx 5 \times 10^{12}$ antiprotons per year are used at CERN. The Fermilab Accumulator routinely provides $\approx 6 \times 10^{12}$ antiprotons per day for the collider program; production rates have now reached nearly 3×10^{11} antiprotons per hour. The FAIR project in Germany is proposed to be an accelerator facility that will share time producing antiprotons and radioactive beams; the antiproton production-rate goal is 10% of what is now being collected by the Fermilab Accumulator. For the medium-energy program considered here, we next discuss how to operate the Fermilab Antiproton Source to maximize the physics reach.

2.1 Future Capabilities, Fill Cycle, and Integrated Luminosity

Currently, the Main Injector minimum cycle time is set at 2.2 s in order to load protons and ramp. In the NOνA era, the Recycler Ring will provide protons in one turn; then the minimum Main Injector cycle time will consist of just the ramp time, 1.33 s. The Antiproton Source is not capable of running at that cycle time and would take proton beam on target every other Main Injector cycle. Currently, when Switchyard is taking beam, the average cycle time for antiproton production is 2.42 s, which is close to the foreseen 2.66 s. The antiproton stacking rate is still $> 2.5 \times 10^{11}$ antiprotons per hour even with Switchyard running. Even though the stacking rate decreases with stack size, we expect

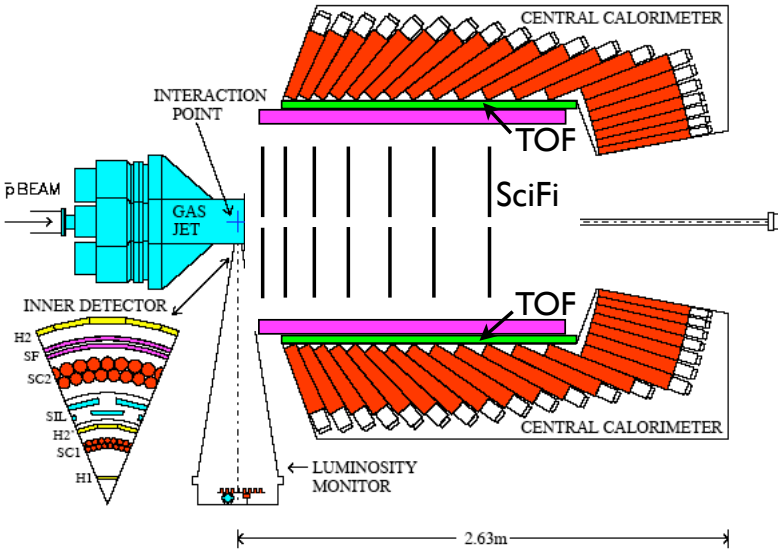

Figure 1: Apparatus configuration assumed for the studies described here: inserted into the bore of the E835 lead-glass barrel calorimeter is a small superconducting solenoid (magenta) containing precision scintillating-fiber tracking detectors. Precision time-of-flight counters (green) surround the solenoid. (If necessary, a return yoke, configured so as to fit under the ceiling of the AP50 pit, could be used to minimize stray field at the lead-glass phototubes; alternatively, a self-shielding double solenoid [1] could be employed.)

to accumulate 10^{12} antiprotons in five hours. The most that E835 decelerated successfully was 10^{12} antiprotons.

The time to prepare the beam (deceleration, energy check and cooling) will be the same as it was for E835. Preparation of the beam for the experiment and stacking are expected to take a few hours.

With a higher-density hydrogen gas jet than E835, the experiment can expect luminosities of $1 - 2 \times 10^{32}$ cm^{-2}s^{-1}. Depending upon the desired energy for running, we expect the beam lifetime to be 10–20 hours.

A nominal run plan could consist of a day-long cycle of stacking, beam preparation, data taking and recovery. We can expect to achieve ≈ 8 pb^{-1} per day and > 200 pb^{-1} per month.

2.2 Scanning

The precision with which the antiproton beam energy can be determined makes the Accumulator a highly precise spectrometer. The narrow beam energy spread allows measurement of narrow resonance line shapes. The beam energy spread is dependent upon the Accumulator lattice and the beam energy; the spread is on the order of a few hundred keV. The beam energy is stepped through a series of energies and the numbers of events are counted per integrated luminosity. Depending upon the production rate of a resonance and the final-state branching fraction, the beam energy is stepped every antiproton fill, or several points of a scan are done with a single beam fill. For example, for the χ_c states, E835

Table 1: Key detector parameters used in simulations

Parameter	value	unit
Target (D study):		
material	Al	
configuration	wire	
diameter	30	μm
Target (X study):		
material	H	
configuration	cluster jet	
Beam pipe:		
material	Be	
diameter	5	cm
thickness	350	μm
Solenoid:		
length	1.6	m
inner diameter	90	cm
field	1	T
SciFi detectors:		
total thickness per doublet	360	μm
fiber pitch	272	μm
fiber diameter	250	μm
number of stations	8	
number of views	3	
number of channels	$\approx$90,000	

observed 30 χ_{c0} and 1000 $\chi_{c1,2}$ $J/\psi\gamma$ events per pb^{-1} when the beam energy corresponded exactly to the appropriate χ_c mass.

The observed line shape is a convolution of the beam energy spread and the natural resonance shape. For the χ_c states, there is no distortion of the resonance shape since the beam energy spread is less than a χ_c width. For resonance widths nearly the same as (or smaller than) the beam energy spread, the shape is distorted with respect to the natural resonance shape. As the resonance width decreases, the observed peak height decreases and the line-shape width approaches the beam energy spread. Two examples from E835 are the reduction of the number of observed events per integrated luminosity by factors of 2 and 5 for the ψ' and J/ψ, respectively, when compared to what would be expected if the beam energy were a delta function. The distortion of line shape has been discussed by the E835 [2] and PANDA collaborations [3].

If the exact mass and width are not known, the beam narrowness can be a hindrance in finding the resonance. If the mass is *known* to a few MeV or so, the width is on the order of a hundred keV, and the expected peak number of events is several per pb^{-1}, then a systematic stepping of energy over several weeks (one energy point per day) may be needed to find the resonance. Once the resonance is found, further energy points are used to determine the mass, width, and background.

Table 2: Experimental observations of $X(3872)$.

Experiment	Year	Mode	Events	Ref.
Belle, BaBar	2003, 2004	$\pi^+\pi^- J/\psi$	35.7 ± 6.8, 25.4 ± 8.7	[4, 7]
CDF, DØ	2004	$\pi^+\pi^- J/\psi$	730 ± 90, 522 ± 100	[5, 6]
Belle	2004	$\omega(\pi^+\pi^-\pi^0)J/\psi$	10.6 ± 3.6	[10]
Belle	2005	$\gamma J/\psi$	13.6 ± 4.4	[8]
Belle	2006	$D^0\overline{D}^0\pi^0$	23.4 ± 5.6	[11]
BaBar	2008	$\gamma\psi$, $\gamma\psi'$	23.0 ± 6.4,25.4 ± 7.3	[9]
BaBar	2008	$D^0\overline{D}^0\pi^0$	33 ± 7	[12]

3 $X(3872)$

The $X(3872)$ was discovered in 2003 by the Belle Collaboration [4] via the decay sequence $B^\pm \to K^\pm X(3872)$, $X(3872) \to \pi^+\pi^- J/\psi$; its existence was quickly confirmed by CDF [5], DØ [6], and BaBar [7]. It has now been seen as well in the $\gamma J/\psi$ [8, 9], $\gamma\psi'$ [9], $\pi^+\pi^-\pi^0 J/\psi$ [10], and $D^0\overline{D}^{*0}$ ($D^0\overline{D}^0\pi^0$, $D^0\overline{D}^0\gamma$) [11, 12, 13] modes (see Table 2). The mass difference between the $J/\psi\pi^+\pi^-$ and the $D^0\overline{D}^{*0}$ decay channels hinted at the possibility of two nearby states. The $X(3872)$ does not appear to fit within the charmonium spectrum. The observed partial width of the state in the $\pi^+\pi^- J/\psi$ decay channel was measured by Belle to be $< 2.3\,\mathrm{MeV}$ at 90% C.L. [4] and by BaBar to be $< 3.3\,\mathrm{MeV}$ at 90% C.L. [14]. The observed partial width of the state in the $D^0\overline{D}^{*0}$ decay channel was measured by BaBar to be $3.0^{+1.9}_{-1.4} \pm 0.9$ MeV [15, 12]. Since the measured mass is well above the open-charm threshold, the small width implies that decays to $D\overline{D}$ are forbidden and suggests unnatural parity, $P = (-1)^{J+1}$ [16]. The $X(3872)$ is a poor candidate for the $\psi_2\,(1\,^3D_2)$ or $\psi_3\,(1\,^3D_3)$ charmonium levels [17, 10, 16] due to the nonobservation of radiative transitions to χ_c. The evidence for $X(3872) \to \gamma J/\psi$ implies positive C-parity, and additional observations essentially rule out all possibilities other than $J^{PC} = 1^{++}$ [18, 19]. With those quantum numbers, the only available charmonium assignment is $\chi'_{c1}\,(2\,^3P_1)$; however, this is highly disfavored [17, 16] by the observed rate of $X(3872) \to \gamma J/\psi$. In addition, the plausible identification of $Z(3930)$ as the $\chi'_{c2}\,(2\,^3P_2)$ level suggests [17] that the $2\,^3P_1$ should lie some $49\,\mathrm{MeV}/c^2$ higher in mass than the observed $m_X = 3872.2 \pm 0.8\,\mathrm{MeV}/c^2$ [15].

Inspired by the coincidence of the $X(3872)$ mass and the $D^0\overline{D}^{*0}$ threshold, a number of ingenious solutions to this puzzle have been proposed, including an S-wave cusp [20] or a tetraquark state [21]. Perhaps the most intriguing possibility is that the $X(3872)$ represents the first clear-cut observation of a meson-antimeson molecule: specifically, a bound state of $D^0\overline{D}^{*0} + D^{*0}\overline{D}^0$ [22].[1] A key measurement is then the precise mass difference between the X and that threshold; if the molecule interpretation is correct, it should be very slightly negative, in accord with the small molecular binding energy [19]:

$$0 < E_X = (m_{D^0} + m_{D^{*0}} - m_X)c^2 \ll 10\,\mathrm{MeV}\,.$$

A direct and precise measurement of the full width, which $\overline{p}p$ can provide [23, 24, 25], is also highly desirable.

[1] Alternatively, the mass coincidence may be merely accidental, and the $X(3872)$ a $c\bar{c}$-gluon hybrid state; however, the mass and 1^{++} quantum numbers make it a poor match to lattice-QCD predictions for such states [17].

With the current world-average values [15] $m_{D^0} = 1864.84 \pm 0.17\,\mathrm{MeV}/c^2$ and $m_{D^{*0}} - m_{D^0} = 142.12 \pm 0.07\,\mathrm{MeV}/c^2$, the $D^0\overline{D}^{*0}$ mass threshold is $3871.8 \pm 0.35\,\mathrm{MeV}/c^2$. Using the world-average value for the mass of the $X(3872)$, we have $E_X = -0.4 \pm 0.8\,\mathrm{MeV}$. If we use for the mass of the $X(3872)$ the most precise single measurement to date (by CDF [26] in the $\pi^+\pi^- J/\psi$ channel), $3871.61 \pm 0.16 \pm 0.19\,\mathrm{MeV}/c^2$, E_X becomes -0.19 ± 0.43 MeV. A future increase in precision of this comparison will also require improvements in the precision of the D^0 and D^{*0} masses. By taking advantage of the small momentum spread and precise momentum-calibration capability of the Antiproton Accumulator, a $\overline{p}p \to X(3872)$ formation experiment can make extremely precise ($\lesssim 100\,\mathrm{keV}/c^2$) measurements of m_X, and directly measure Γ_X to a similar precision, by scanning across the resonance as discussed above. Since the mass of the $X(3872)$ is so close to the $D^{*0}\overline{D}^{*0}$ threshold, mapping precisely the lineshape of the X will be necessary in determining whether we have a single state or two distinct, nearby states with different masses. The B factories could attempt to measure the line shape but this is an extremely challenging measurement for them due to low statistics and relatively poor resolution [27]. The $\overline{p}p$ experiment can uniquely perform this line shape measurement both below and above the $D^0\overline{D}^{*0}$ threshold. This is the type of measurement for which the $\overline{p}p$ scanning technique has a demonstrated strong advantage.

Additional important measurements include $\mathcal{B}[X(3872) \to \pi^0\pi^0 J/\psi]$ and study of the $\pi^0\pi^0$ mass spectrum which will help confirm the C-parity assignment [28] and test the $\rho J/\psi$ production hypothesis. These measurements are very hard for the current B factories due to machine-related backgrounds and low efficiency to detect the π^0's when one tries to reduce the combinatorial background from low-energy photons. The experiment proposed here (as well as BES-III) could attempt to measure with better precision ($\sim 100\,\mathrm{keV}/c^2$) the D^0 mass as well, using a $\psi(3770) \to D^0\overline{D}^0$ sample [29], and thus determine better the $D^0\overline{D}^{*0}$ threshold. (A $\overline{p}p$ experiment could also scan the $3.92 < \sqrt{s} < 3.94\,\mathrm{GeV}$ region to study the resonance observed recently in the $J/\psi\omega$ decay mode [30], as well as investigating the other charmonium-like states observed in this vicinity [31].)

3.1 $X(3872)$ Sensitivity Estimate

The production cross section of $X(3872)$ in $\overline{p}p$ annihilation has not been measured, but it has been estimated to be similar in magnitude to that of the χ_c states [32, 33]. In E760, the χ_{c1} and χ_{c2} were detected in $\overline{p}p \to \chi_c \to \gamma J/\psi$ (branching ratios of 36% and 20%, respectively [15]) with acceptance times efficiency of $44 \pm 2\%$, giving about 500 observed events each for an integrated luminosity of $1\,\mathrm{pb}^{-1}$ taken at each resonance; at the mass peak 1 event per nb^{-1} was observed [34]. The lower limit $\mathcal{B}[X(3872) \to \pi^+\pi^- J/\psi] > 0.042$ at 90% C.L. [35] implies that in a day (section 2.1) at the peak of the $X(3872)$ ($8\ \mathrm{pb}^{-1} \times [1000\ \mathrm{events}/\mathrm{pb}^{-1}] \times 0.04/0.36 \times$ acceptance-efficiency ratio of final states of $\approx 50\%$), about 500 events would be observed. Even if the production cross section is an order of magnitude less than those of the χ_c states, the tens of events per day at the peak will be greater than the background observed by E835. By way of comparison, Table 2 shows current sample sizes, which are likely to increase by not much more than an order of magnitude as these experiments complete during the current decade.[2] (Although CDF and DØ could amass samples of order 10^4 $X(3872)$ decays, the large backgrounds in the CDF and DØ observations, reflected in the uncertainties on the numbers of events listed in Table 2, limit their incisiveness.)

[2]The $\overline{p}p \to X(3872)$ sensitivity will be competitive even with that of the proposed SuperKEKB [36] upgrade, should that project go forward.

The spread of reported $X(3872)$ masses means that a range of > 6 MeV will need to be scanned. If the observations attributed to the $X(3872)$ are two resonances or a threshold effect, the step sizes will have to be less than the beam spread (section 2.2) to see a narrow resonance and investigate the threshold. A systematic program of stepping of energies through the large mass range may be necessary to establish the line shape(s), which could take two months.

We have concentrated here on one decay mode of the $X(3872)$: $X(3872) \to \pi^+\pi^- J/\psi$. Large samples will of course also be obtained in other modes as well, increasing the statistics and allowing knowledge of $X(3872)$ branching ratios to be improved. Given the uncertainties in the cross section and branching ratios, the above may well be an under- or overestimate of the $\overline{p}p$ formation and observation rates, perhaps by as much as an order of magnitude. Nevertheless, it appears that a new experiment at the Antiproton Accumulator could obtain the world's largest clean samples of $X(3872)$, in perhaps as little as a month of running. The high statistics, event cleanliness, and unique precision available in the $\overline{p}p$ formation technique could enable the world's smallest systematics. Such an experiment could thus provide a definitive test of the nature of the $X(3872)$.

4 Charm

There are several potential signatures for new physics in charm mixing and decay; these have been comprehensively reviewed in (*inter alia*) the Proceedings of the 2007 "Workshop on Flavour in the Era of the LHC" [37]. As emphasized by many authors, these have the virtues of unique sensitivity to new physics in the "up-quark" sector, low to nonexistent standard-model background, and availability of very large event samples. They include rare (flavor-changing neutral-current or lepton-flavor violating) decays, and both direct and indirect *CP* asymmetries. Charm mixing is now established at the $\approx 10\sigma$ level [38], but is in a range $(x_D, y_D \lesssim 1\%)$ such that its interpretation is ambiguous: mixing at that level could arise from the standard model or from new physics. Nevertheless it is important to study D^0 mixing as precisely possible as well as to look for signatures of new physics via *CP* violation and rare decays. These can be complex analyses, so for now we have used as a simple benchmark the numbers of events reconstructed in the tagged D^0 decay modes $D^{*+} \to D^0\pi^+ \to (K^-\pi^+)\pi^+$ and $D^{*-} \to \overline{D}^0\pi^- \to (K^+\pi^-)\pi^-$.

4.1 $D^{*\pm} \to D^0$ Study

We have simulated the exclusive reaction $\overline{p}n \to D^{*-}D^0$, with subsequent decays $D^{*-} \to \pi_s^-\overline{D}^0$, $\overline{D}^0 \to K^+\pi^-$, at 8 GeV $\overline{p}$ kinetic energy. (This is the design energy of the Antiproton Accumulator, and also essentially its maximum practical operating energy. As shown by Braaten [33] and Titov and Kämpfer [39], this is also approximately the energy at which the exclusive $\overline{p}N \to D^*D$ cross section peaks.) We assume uniform production- and decay-angle distributions. We find that the acceptance for tagged-D^0 events (i.e., for the slow pion from the D^* and the kaon and pion from the D^0 all to be detected), about 45%, is largely insensitive to spectrometer magnetic field (Fig. 2). (The exact value of the acceptance is of course sensitive to size and placement of detectors; we find that the configuration given in Table 1 is a reasonable compromise between acceptance and detector channel count.)

Figure 3 shows the transverse-momentum (p_t) distributions of the charged pions from this decay sequence. The pion p_t distributions are non-overlapping, which means that there is essentially no ambiguity as to which pion is from the D^* and which from the D^0.

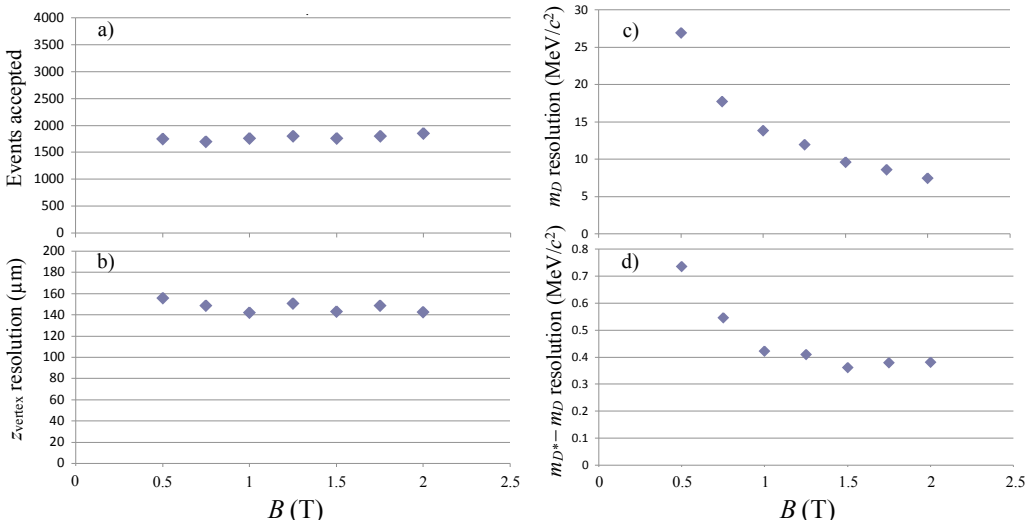

Figure 2: Magnetic-field dependence of a) number of events accepted (out of 4,000 thrown), b) decay-distance resolution, c) D^0 mass resolution, and d) D^*–D^0 mass-difference resolution. Above ≈ 1 T, spectrometer performance improves only slightly.

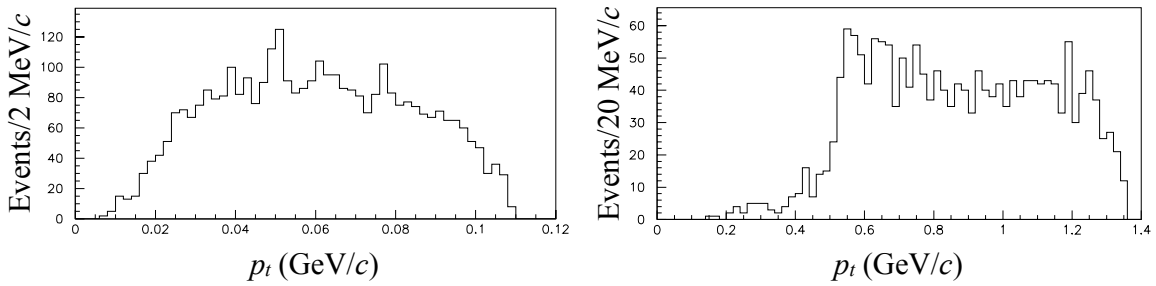

Figure 3: Transverse-momentum (p_t) histograms for charged pions from accepted tagged-D^0 events. The "slow" (left histogram) and "fast" pions (right histogram) are seen to have non-overlapping p_t distributions, thus there is no ambiguity in event reconstruction as to which is which. (The p_t distribution of the kaon is similar to that of the fast pion.)

However, the D^0 kaon and pion have very similar p_t distributions, hence kaon identification will be important if large signal-to-background ratio is to be achieved. Figure 4 shows the resolutions achieved in D^* and D^0 mass, D^*–D^0 mass difference, and D^0 decay distance at a magnetic field of 1 T. Since these events have no primary vertex, in computing the decay distance we rely on the small size of the target in at least one (z) dimension.

4.2 *D* Background Study

To estimate the efficiency of the cuts needed for good signal-to-background in tagged-D^0 decays, we have analyzed the MIPP 20 GeV/c data sample [40]. Approximately 30,000 events were reconstructed in MIPP with 3 or more charged tracks produced by a 20 GeV/c antiproton incident on a liquid-hydrogen target. These correspond to a total $\geq$ 3-prong production cross section of about 30 mb, hence the sensitivity of the sample is about 1 event/μb. The events are a mixture of interactions in the liquid hydrogen, the aluminum target-vessel win-

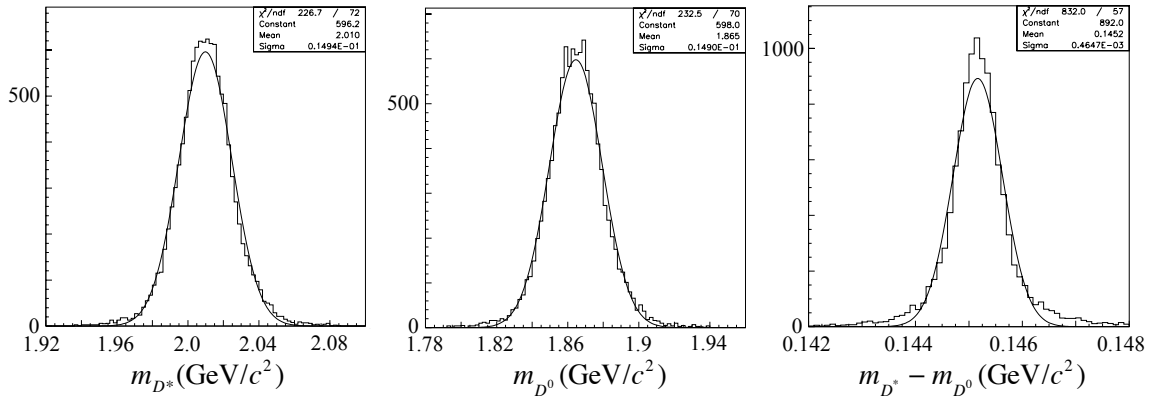

Figure 4: (left to right) Histograms of D^* and D^0 mass, and D^*-D^0 mass difference, indicating r.m.s. resolutions of 14.9, 14.9, and 0.46 MeV/c^2, respectively.

dows, and the plastic interaction-trigger scintillation counter. Because these events are in an awkward momentum range for hadron identification, with most hadrons above the dE/dx particle-identification ($p < 0.5\,\mathrm{GeV}/c$) range and below that of the the MIPP Cherenkov counter ($p > 5\,\mathrm{GeV}/c$), hadron-ID information was not used in this analysis.

We first scaled the longitudinal momentum of each track by a factor of 0.65 in order to correct (to first order) for the higher beam momentum in the MIPP sample than in 8 GeV collisions. This correction was derived by comparing the momentum distributions of the decay products in simulated $D^* \to D^0$ events at 20 and 8 GeV. This procedure is conservative in that in actual 8 GeV collisions, transverse momenta and event charged-particle multiplicities would also be reduced compared to those in the MIPP sample, but we made no attempt to correct for these effects.

For a subset of events, Cherenkov information was available and was used to eliminate the large fraction of electrons and positrons. We then computed "D^*" and "D^0" masses, assuming $\pi^{\mp}K^{\pm}\pi^{\mp}$ track identities, for every $-+-$ and $+-+$ charge-sign triple of charged tracks in each event, requiring $p_{t1} < p_{t2}, p_{t3}$ (where particle 1 is taken as the "slow" pion coming from the D^* decay) in accordance with the Monte Carlo distributions of Fig. 3. Figure 5 shows the distribution of events vs. these reconstructed masses, and Fig. 6 shows the distributions of D^*–D^0 mass difference for all events and for those events in which the D^* and D^0 masses are consistent with the known masses of those particles. Note the power of the D^* and D^0 mass cuts in eliminating background combinations: in Fig. 6(right) there is only one event remaining in the (1-MeV-wide) signal mass-difference bin, $m_{D^*} - m_{D^0} = 0.145\,\mathrm{GeV}/c^2$. We therefore conclude that the background level, before hadron-ID and vertex requirements are imposed, will be about 1 μb. (Note that insofar as our sample probably still contained many leptons, this gives an approximate upper limit.)

To get an idea of the signal-to-background ratio, we assume a total $D^{*\pm}$ production cross section (including both signs and taking into account the $A^{0.29}$ enhancement factor due to target material [41]) of 10 μb in 8 GeV $\overline{p}p$ collisions (see Table 3). We thus start out (before branching ratios are taken into account) with a signal-to-background ratio of about 10 to 1. The decay chain for the final state we consider here involves the $(67.7 \pm 0.5)\%$ $D^{*+} \to \pi^+ D^0$ branching ratio and the $(3.89 \pm 0.05)\%$ $D^0 \to K^-\pi^+$ branching ratio [42], reducing the signal-to-background ratio to 1/4. However, based on multiplicities observed in bubble-chamber experiments [43], the charged-kaon production rate at 8 GeV is $\lesssim 0.1$ per

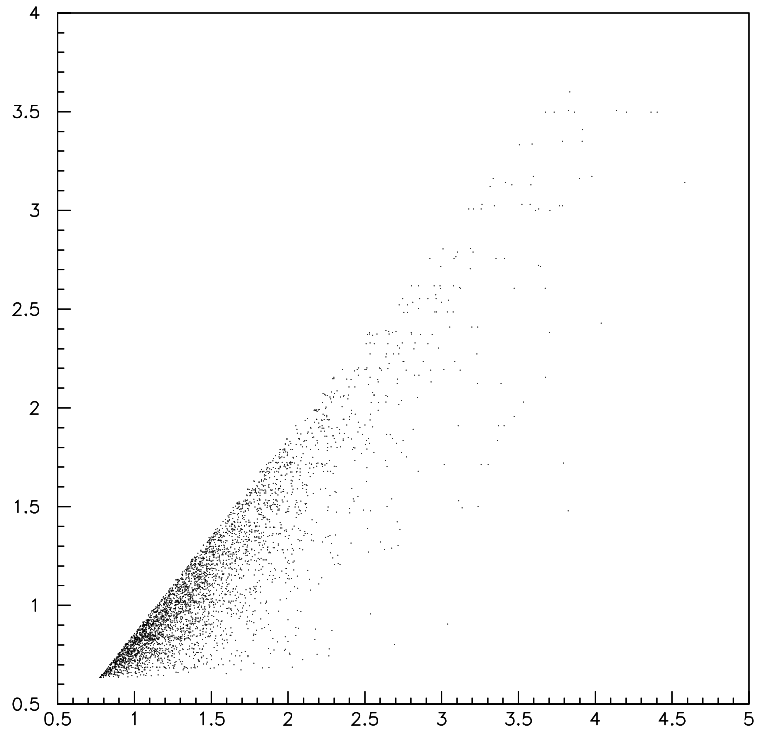

Figure 5: Scatter plot of reconstructed "$D^0 \to K\pi$" vs. "$D^{*\pm} \to \pi^{\pm}(\overline{D}{}^0)0$" masses (in GeV/$c^2$) as described in text. (In order to avoid saturating the scatter plot, only a fraction of the events are plotted.)

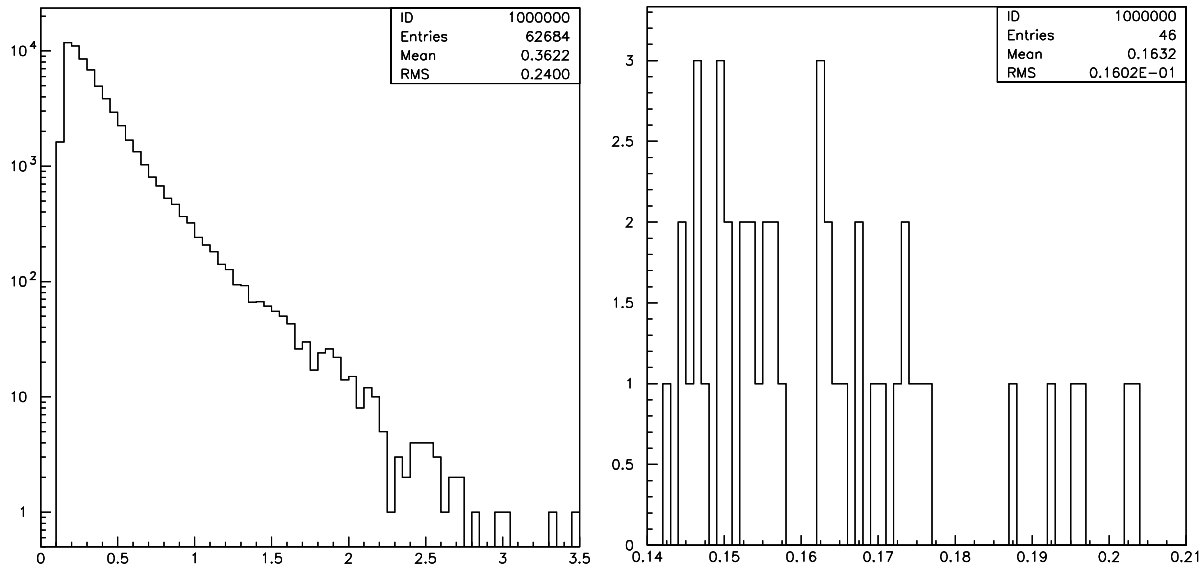

Figure 6: D^*–D mass-difference distributions (in GeV/c^2): (left) all events; (right) events within $\pm 2\sigma$ D^* and D mass windows.

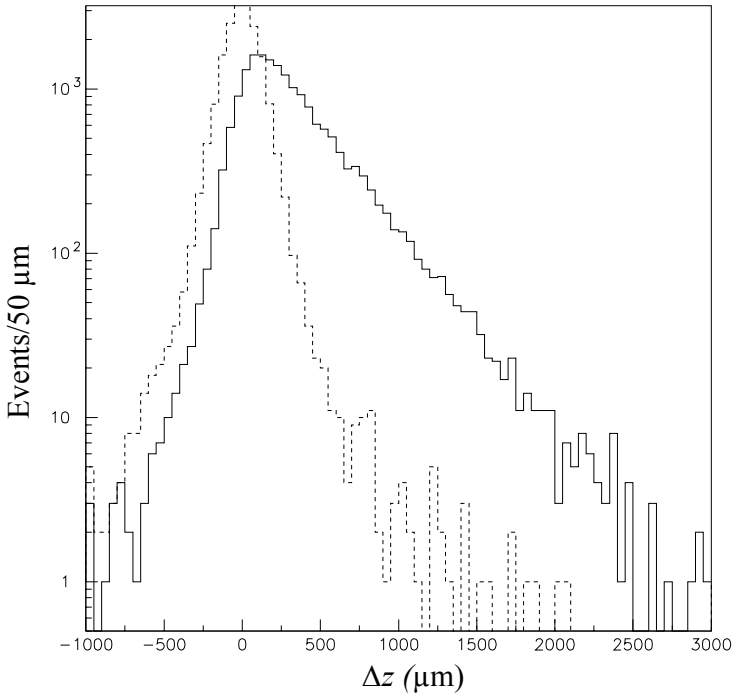

Figure 7: Histograms of reconstructed vertex position for D^0 decays (solid) and random hadron pairs (dashed).

event, thus a factor of 10 or more is available from hadron identification (see below), giving a signal-to-background of ≈ 10 to 1. To achieve signal-to-background of 100 to 1 or more would then require lifetime cuts (Fig. 7). (Note that the lifetime resolution we obtain is based solely on the use of fine-pitch scintillating-fiber detectors. It may be possible to do somewhat better with silicon detectors but the trade-off of finer pitch vs. increased multiple scattering must be handled with care, and so far the all-SciFi solution presented here gives the best performance of those options examined.)

4.3 Kaon Identification

We assume π-K discrimination by means of precision time-of-flight measurement. (An alternative would be the DIRC technique developed for BaBar.) A time measurement precision of ≈ 50 ps is typical using scintillation counters of few-cm thickness [44], however, this does not suffice for π-K discrimination at the level we need (Fig. 8). Devices with resolution better than 10 ps are in development [45] and are likely to be available on the timescale of this experiment.

4.4 Charm Sensitivity Estimate

Table 3 (repeated verbatim from P-986 Addendum 1 [41]) gives expected produced and reconstructed samples of 2.1×10^{10} and 2.7×10^{7} tagged events per year. This is consistent with the luminosity estimate given in Sec. 2.1 above: 8 pb^{-1}/day amounts to 2,920 pb^{-1}/year, compared to the 3,200 pb^{-1}/year implied by Table 3, whereas the integrated luminosity running at 8 GeV (for which no deceleration is required) will be somewhat higher than that

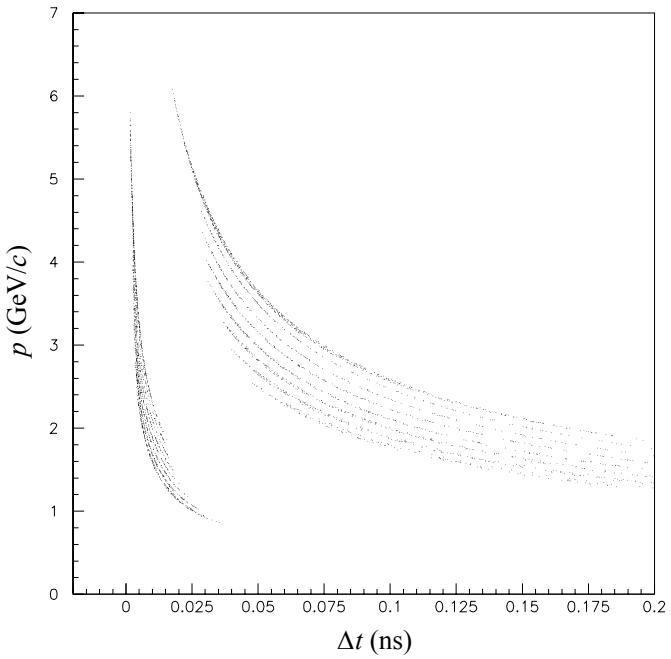

Figure 8: Momentum vs. time-of-flight difference (at last hit SciFi plane) for fast pion and kaon from simulated D^0 decays in 8 GeV $\bar{p}p$ collisions. At all momenta, a 10 ps r.m.s. resolution in Δt provides at least 2σ separation; for most of the range the separation is $\geq 3\sigma$.

at the mass of the $X(3872)$ (for which the antiprotons need to be decelerated to 6.1 GeV). The other difference between Table 3 and the discussion here is that the acceptance is about 10% smaller than previously assumed — not an important difference given the much larger cross-section uncertainties.

We have focused here on the simplest decay modes, but we anticipate correspondingly large samples of other charm decays, including $D^+ \to K^-\pi^+\pi^+$ and $D^0 \to K_S\pi^+\pi^-$, singly and doubly Cabibbo-suppressed modes such as K^+K^-, $\pi^+\pi^-$, $K^+\pi^-$, etc. In contrast to certain other experiments, these will be free of all contamination from the more complicated event topologies of $B \to D$ decays.

One important benchmark for new-physics reach in charm is leptonic decays; an example is $D^0 \to \mu^+\mu^-$, whose branching ratio in the standard model (SM) has been estimated as $\sim 3 \times 10^{-13}$, but can be enhanced by new physics to as much as $\sim 4 \times 10^{-7}$ [37], possibly observable in BES-III as well as LHC*b*. The best current limit, 4.3×10^{-7} from CDF, already constrains SUSY models [46]. With some 2×10^{10} charm events produced and acceptance $\times$ efficiency ~ 0.05, our sensitivity could rival or exceed the 3×10^{-8} (at 90% C.L.) estimated for BES-III [37]. However, more work will be required (and is in progress) to assess the likely pion rejection from the TOF and calorimeter. Similar statements apply as well for other FCNC or LFV modes such as $K\mu\mu$, Kee, $K\mu e$, etc. For all of these modes, the best limit from any approved experiment is expected to come from BES-III and to be statistics (not systematics) -limited. In comparison, based on the assumptions used here, per year of operation, our proposed experiment will amass some 27 times the statistics of BES-III.

The benchmark emphasized in our previous note [41] was sensitivity to new physics via

Table 3: Assumed values and sensitivity-benchmark estimate of tagged ${}^{(}\overline{D}{}^{)}0 \to K^{\mp}\pi^{\pm}$ events per year. (Caveats: As discussed in text, the reliability of some of these values remains to be established. They are based on exclusive cross-section estimates, so the inclusive production rate could be significantly higher, but the cross section, luminosity, or efficiency could also be lower.) (From P-986 Addendum 1, "Antiproton Annihilation and Open Charm" [41]).

Quantity	Value	Unit
Running time	2×10^7	s/y
Duty factor	0.8*	
$\mathcal{L}$	2×10^{32}	$\mathrm{cm}^{-2}\mathrm{s}^{-1}$
Target A	27	
$A^{0.29}$	2.6	
$\sigma(\overline{p}p \to D^{*+}X)$	1.25	μb
# $D^{*\pm}$ produced	2.1×10^{10}	events/y
$\mathcal{B}(D^{*+} \to D^0\pi^+)$	0.677	
$\mathcal{B}(D^0 \to K^-\pi^+)$	0.0389	
Acceptance	0.5	
Efficiency	0.1	
Total	2.7×10^7	events/y

*Assumes $\approx$15% of running time is devoted to antiproton-beam stacking.

charm *CP* violation, where partial-width sensitivities of 10^{-3} to 10^{-4} in Cabibbo-favored, and 1% in doubly-Cabibbo-suppressed, modes are of interest for detecting new physics, and, for time-dependent *CP* asymmetries, 10^{-4} and 10^{-3} in Cabibbo-favored and doubly Cabibbo-suppressed modes, respectively [37]. A sample of 2×10^7 reconstructed events in the Cabibbo-favored $D^0 \to K^-\pi^+$ mode does indeed probe partial widths at the few $\times 10^{-4}$ statistical level; however, at that level of precision, systematics will be paramount. A typical strategy has been to use any apparent asymmetry observed in the $K^{\mp}\pi^{\pm}$ mode instead as a measure of apparatus bias, and focus on the *normalized* doubly Cabibbo-suppressed partial-rate asymmetry,

$$\frac{\Gamma(D^0 \to K^+\pi^-) - \Gamma(\overline{D}{}^0 \to K^-\pi^+)}{\Gamma(D^0 \to K^-\pi^+) - \Gamma(\overline{D}{}^0 \to K^+\pi^-)} \, .$$

The uncertainty of this ratio should be dominated by the statistical uncertainty of the numerator, or 0.7% for 8×10^4 "wrong-sign" ${}^{(}\overline{D}{}^{)}0 \to K^{\pm}\pi^{\mp}$ reconstructed (corresponding to 2×10^7 observed, tagged, "right-sign" ${}^{(}\overline{D}{}^{)}0 \to K^{\mp}\pi^{\pm}$ events). The sensitivity will be further increased due to additional wrong-sign modes that will be observed, but could be worse if the charm cross section is smaller than assumed or if more stringent cuts than assumed are required in order to suppress background.

We hope to address these issues further in our oral presentation.

5 Conclusions

Further study bears out our contention that the experiment we propose is potentially capable of reconstructing the world's largest charm samples and making a high-impact measure-

ment: the first observation of new physics in charm CP violation. It also has the potential to make the world's most precise measurements of the properties of the $X(3872)$, and to shed light on the mystery of that state's makeup and nature. These are examples of the broad physics program that can be carried out with a high-rate magnetic spectrometer at the world's best antiproton source.

We request support from Fermilab to proceed to a detailed study, including a more thorough and detailed program of simulations and evaluation of the cost of mounting and operating the experiment.

References

[1] I.e., two nested solenoid windings, with opposite polarity, in one cryostat; see e.g. K. Sinokita, R. Toda, and Y. Sasaki, J. Phys.: Conf. Ser. **150**, 012041 (2009) and references therein.

[2] M. Andreotti *et al.*, Phys. Lett. B **654**, 74 (2007).

[3] M. F. M. Lutz *et al.*, "Physics Performance Report for PANDA: Strong Interaction Studies with Antiprotons," arXiv:0903.3905 [hep-ex] (2009).

[4] S. K. Choi *et al.* [Belle Collaboration], Phys. Rev. Lett. **91**, 262001 (2003).

[5] D. Acosta *et al.* [CDF II Collaboration], Phys. Rev. Lett. **93**, 072001 (2004).

[6] V. M. Abazov *et al.* [DØ Collaboration], Phys. Rev. Lett. **93**, 162002 (2004).

[7] B. Aubert *et al.* [BABAR Collaboration], Phys. Rev. D **71**, 071103 (2005).

[8] K. Abe *et al.* [Belle Collaboration], "Evidence for $X(3872) \to \gamma J/\psi$ and the sub-threshold decay $X(3872) \to \omega J/\psi$," arXiv:hep-ex/0505037.

[9] B. Aubert *et al.* [BABAR Collaboration], arXiv:0809.0042v1 [hep-ex].

[10] K. Abe *et al.* [Belle Collaboration], arXiv: hep-ex/0408116.

[11] G. Gokhroo *et al.* [Belle Collaboration], Phys. Rev. Lett. **97**, 162002 (2006).

[12] B. Aubert *et al.* [BABAR Collaboration], Phys. Rev. D **77**, 011102R (2008).

[13] I. Adachi *et al.* [Belle Collaboration], arXiv:hep-ex/0809.1224.

[14] B. Aubert *et al.* [BABAR Collaboration], Phys. Rev. D **77**, 111101R (2008).

[15] C. Amsler *et al.* [Particle Data Group], Phys. Lett. B **667**, 1 (2008).

[16] N. Brambilla *et al.* [Quarkonium Working Group], *Heavy Quarkonium Physics*, CERN Yellow Report CERN-2005-005 (2005).

[17] E. Eichten. K, Lane, and C. Quigg, Phys. Rev. D **73**, 014014 (2006); Erratum-*ibid.* D **73**, 079903 (2006).

[18] K. Abe *et al.* [Belle Collaboration], "Experimental constraints on the possible J^{PC} quantum numbers of the $X(3872)$," contributed to *22nd International Symposium on Lepton-Photon Interactions at High Energy (LP 2005)*, Uppsala, Sweden, 30 June – 5 July 2005, arXiv:hep-ex/0505038.

[19] E. Braaten, "Review of the $X(3872)$," presented at the *Int. Workshop on Heavy Quarkonium – 2006*, Brookhaven National Laboratory, June 27–30, 2006; available from
`http://www.qwg.to.infn.it/WS-jun06/WS4talks/Tuesday_AM/Braaten.pdf`

[20] D. V. Bugg, Phys. Lett. B **598**, 8 (2004); Phys. Rev. D **71**, 016006 (2005).

[21] L. Maiani, F. Piccinini, A. D. Polosa, and V. Riquer, Phys. Rev. D **71**, 014028 (2005); L. Maiani, V. Riquer, F. Piccinini and A. D. Polosa, Phys. Rev. D **72**, 031502 (2005); H. Hogaasen, J. M. Richard and P. Sorba, Phys. Rev. D **73**, 54013 (2006).

[22] N. A. Tørnqvist, Phys. Lett. B **590**, 209 (2004).

[23] G. Garzoglio *et al.* [E835 Collaboration], Nucl. Instrum. Meth. A **519**, 558 (2004).

[24] T. A. Armstrong *et al.* [E835 Collaboration], Phys. Rev. D **47**, 772 (1993).

[25] See `http://www.e835.to.infn.it/`

[26] The CDF II Collaboration, http://www-cdf.fnal.gov, Public Note 9454, or `http://www-cdf.fnal.gov/physics/new/bottom/bottom.html`.

[27] See e.g. discussion by B. Yabsley at the "International Workshop on Heavy Quarkonia 2008," 2–5 December 2008, Nara Women's University, Nara, Japan, `http://www-conf.kek.jp/qwg08/`.

[28] T. Barnes, S. Godfrey, Phys. Rev. D **69**, 054008 (2004).

[29] C. Cawlfield *et al.* [CLEO Collaboration], Phys. Rev. Lett. **98**, 092002 (2007) [arXiv:hep-ex/0701016].

[30] K. Abe *et al.* [Belle Collaboration], Phys. Rev. Lett. **94**, 182002 (2005).

[31] See e.g. E. Eichten, in "Round table on XYZ and states close to threshold," presented at "International Workshop on Heavy Quarkonium 2007," 17–20 October 2007, DESY, Hamburg, Germany, `http://www.desy.de/qwg07/index.php`.

[32] E. Braaten, Phys. Rev. D **73**, 011501(R) (2006).

[33] E. Braaten, Phys. Rev. D **77**, 034019 (2008).

[34] T. A. Armstrong *et al.* [E760 Collaboration], Nucl. Phys. B **373**, 35 (1992).

[35] B. Aubert *et al.* [BABAR Collaboration], Phys. Rev. Lett. **96**, 052002 (2006).

[36] See `http://belle.kek.jp/superb/.`

[37] M. Artuso *et al.*, Eur. Phys. J. C **57**, 309 (2008); arXiv:0801.1833 [hep-ph].

[38] Heavy-Flavor Averaging Group, presented at "34th International Conference on High-Energy Physics (ICHEP08)," July 29th – August 5th, 2008, Phila., PA.

[39] A. I. Titov and B. Kämpfer, Phys. Rev. C **78**, 025201 (2008).

[40] We are grateful to the MIPP collaboration for making these data available to us.

[41] P-986 Collaboration, "P-986 Addendum: Antiproton Annihilation and Open Charm," Feb. 5, 2009.

[42] C. Amsler *et al.* [Particle Data Group], Phys. Lett. **B 667**, 1 (2008).

[43] J. E. Enstrom, T. Ferbel, P. F. Slattery, B. L. Werner, Report LBL-58, May 1972.

[44] See e.g. M. Bonesini, to appear in Proc. 10th International Workshop on Neutrino Factories, Superbeams and Betabeams, June 30 – July 5, 2008, Valencia, Spain; arXiv:0810.0420v1 [physics.ins-det] (2008).

[45] H. Frisch, private communication.

[46] R. Harr (for the CDF Collaboration), presented at the 34th International Conference on High Energy Physics (ICHEP08), Philadelphia, 2008, arXiv:0810.3444 [hep-ex].